

to imines of low inherent nucleophilicity and has led to an extremely concise synthesis of (\pm)lycorine (13 steps from saffrole).

Acknowledgment. We are grateful to the National Institute of General Medical Sciences of the National Institutes of Health for a grant (GM-29290) in support of these studies. We also acknowledge support in the form of NRSA fellowships to S.W.G. (GM-09624) and M.A.W. (GM-10641).

Supplementary Material Available: Spectroscopic and selected analytical data for compounds **5**, **7**, **12**, **14**, **15**, **17**, and **19-23** (3 pages). Ordering information is given on any current masthead page.

Thermal Encapsulation and Photochemical Deencapsulation of Ag(I) by $[\text{Ir}_2(\text{dimen})_4](\text{PF}_6)_2$ (dimen = 1,8-Diisocyanomenthane). X-ray Crystal Structure of $[\text{AgIr}_2(\text{dimen})_4](\text{PF}_6)_3 \cdot 2\text{DMSO}$

Andrew Sykes and Kent R. Mann*

Department of Chemistry, University of Minnesota
Minneapolis, Minnesota 55455

Received May 16, 1988

During the past few years, our group has been studying the electrochemical properties of d^8 - d^8 metal complexes of Rh(I) and Ir(I).¹⁻⁴ These complexes undergo either two one-electron oxidation processes or a single two-electron process that results in the formation of a metal-metal bond. We were surprised that our attempts to generate stable d^8d^7 radical species³ from compounds with long (4.45 Å) metal-metal distances ($[\text{M}_2(\text{dimen})_4](\text{PF}_6)_2$ (M = Rh,⁵ Ir,^{6,7} dimen^{8,9} = 1,8-diisocyanomenthane)), via the addition of the one-electron oxidant Ag^+ , gave Ag^+ adducts instead.¹⁰ We report here our preliminary observations regarding the formation, structure, and properties of the more stable adduct with M = Ir. This remarkable adduct features an encapsulated, two-coordinate Ag^+ ion that deencapsulates on exposure to near ultraviolet light.

The sequential addition of AgPF_6 to CH_3CN solutions of $[\text{Ir}_2(\text{dimen})_4](\text{PF}_6)_2$ results in UV-vis spectral changes consistent

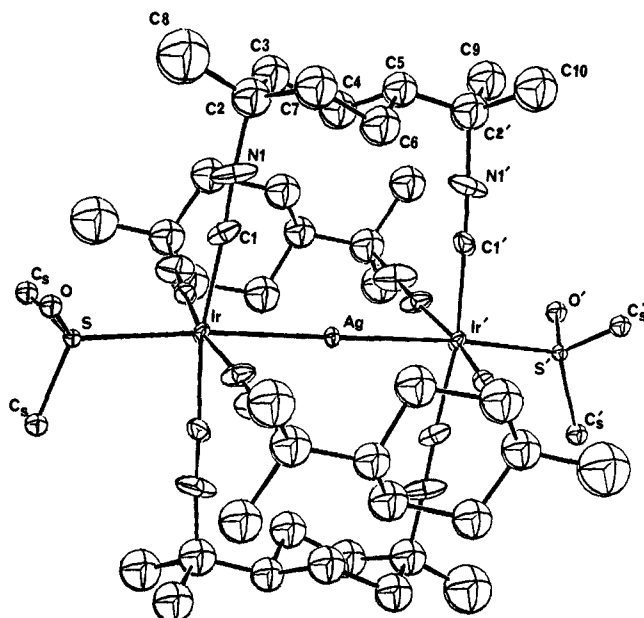


Figure 1. ORTEP view of the $[\text{AgIr}_2(\text{dimen})_4(\text{DMSO})_2]^{3+}$ cation.

with the clean conversion to a single new species. The end point of the spectral changes are reached when 1.0 ± 0.1 equiv of AgPF_6 are added. Rotary evaporation of a similarly prepared acetone solution gives a pale yellow, microcrystalline powder. Elemental analysis indicates that the powder has the composition $[\text{AgIr}_2(\text{dimen})_4](\text{PF}_6)_3 \cdot \text{acetone}$.⁷ Slow recrystallization of the powder from DMSO/ether gave yellow crystals that were the subject of an X-ray structural characterization.^{11,12} An ORTEP illustration of the $[\text{AgIr}_2(\text{dimen})_4(\text{DMSO})_2]^{3+}$ cation is shown in Figure 1.

The structure reveals that the Ag^+ ion has been encapsulated by the Ir_2^{2+} complex to form a linear Ir-Ag-Ir³⁺ unit. The Ir-Ag distances are 2.642 (1) Å and require an Ir-Ir distance of 5.284 Å. No other atoms are within reasonable bonding distances of the Ag^+ , suggesting that the encapsulation reaction is driven by the formation of the Ir³⁺-Ag⁺ interactions and the accompanying solvation changes.

In solution, the $[\text{AgIr}_2(\text{dimen})_4]^{3+}$ cation exhibits a pronounced ability to coordinate ligands in the Ir axial positions. Axial coordination shifts the intense electronic transition that is characteristic of the linear arrangement of metal atoms in $[\text{AgIr}_2(\text{dimen})_4]^{3+}$. For example, solutions of $[\text{AgIr}_2(\text{dimen})_4]^{3+}$ in CH_2Cl_2 exhibit this transition at 390 nm. Addition of acetone, acetonitrile, pyridine, or triphenylphosphine to the solution results in a shift of the absorption band to higher energy. In the cases of pyridine⁷ and triphenylphosphine,⁷ the bis adducts $[\text{AgIr}_2(\text{dimen})_4(\text{L})_2]^{3+}$ have been isolated and characterized.

Several of our preliminary measurements and observations suggest a rich and interesting chemistry for the encapsulated Ag^+ adduct. One point of immediate interest is the magnitude of the Ag^+ encapsulation equilibrium constant. A potentiometric titration¹³ (Figure 2) of a $\text{AgPF}_6/\text{DMSO}$ solution with $[\text{Ir}_2(\text{dimen})_4]^{2+}$ that utilized a Ag metal electrode to monitor $[\text{Ag}^+]$ gives

(1) Rhodes, M. R.; Mann, K. R. *Inorg. Chem.* **1984**, *23*, 2053.
(2) Boyd, D. C.; Rodman, G. S.; Mann, K. R. *J. Am. Chem. Soc.* **1986**, *108*, 1779.

(3) Boyd, D. C.; Matsch, P. A.; Mixa, M. M.; Mann, K. R. *Inorg. Chem.* **1986**, *25*, 3331.

(4) Bullock, J. P.; Boyd, D. C.; Mann, K. R. *Inorg. Chem.* **1987**, *26*, 3084.

(5) (a) Mann, K. R. *Crystal Struct. Commun.* **1981**, *10*, 451. (b) Che, C.-M.; Herbstein, F. H.; Schaefer, W. P.; Marsh, R. E.; Gray, H. B. *Inorg. Chem.* **1984**, *23*, 2572. (c) Gladfelter, W. L.; Lynch, M. W.; Schaefer, W. P.; Hendrickson, D. N.; Gray, H. B. *Inorg. Chem.* **1981**, *20*, 2390. (d) Gladfelter, W. L.; Gray, H. B. *J. Am. Chem. Soc.* **1980**, *102*, 5910.

(6) Smith, T. P. Ph.D. Thesis, California Institute of Technology, **1982**.
(7) New compounds were characterized by ¹H and ¹³C{¹H} NMR, IR, UV-vis, FAB mass spectrometry, and C, H, N elemental analyses. Complete data appear in the microfiche addition as Supplementary Material.

(8) Liptak, A.; Kusiak, J. W.; Pitha, J. *J. Med. Chem.* **1985**, *28*, 1699.

(9) Prepared by a standard method, see: Weber, W. P.; Gokel, G. W.; Ugi, I. K. *Angew. Chem., Int. Ed. Engl.* **1972**, *11*, 530.

(10) A variety of Ag^+ adducts of transition-metal complexes have been reported: (a) Connelly, N. G.; Lucy, A. R.; Galas, A. M. R. *J. Chem. Soc., Chem. Commun.* **1981**, 43. (b) Connelly, N. G.; Lucy, A. R.; Payne, J. D.; Galas, A. M. R.; Geiger, W. E. *J. Chem. Soc., Dalton Trans.* **1983**, 1879. (c) Ladd, J. A.; Hope, H.; Balch, A. L. *Organometallics* **1984**, *3*, 1838. (d) Rhodes, L. F.; Huffman, J. C.; Caulton, K. G. *J. Am. Chem. Soc.* **1984**, *106*, 6874. (e) Rhodes, M. R. Ph.D. Thesis, University of Minnesota, **1984**. (f) Ciriano, M. A.; Oro, L. A.; Pérez-Torrente, J. J.; Tiripicchio, A.; Tiripicchio-Camellini, M. *J. Chem. Soc., Chem. Commun.* **1986**, 1737. (g) Liston, D. J.; Reed, C. A.; Eigenbrot, C. W.; Scheidt, W. R. *Inorg. Chem.* **1987**, *26*, 2740. (h) Balch, A. L.; Ghedini, M.; Oram, D. E.; Reedy, P. E. *Inorg. Chem.* **1987**, *26*, 1223. (i) Uson, R.; Fornies, J.; Thomas, M.; Casas, J. M.; Cotton, F. A.; Falvello, L. R. *Inorg. Chem.* **1987**, *26*, 3482.

(11) Crystallographic data for $[\text{IrAg}(\text{dimen})_4](\text{PF}_6)_3 \cdot 2\text{DMSO}$: MW = 1814.52; orthorhombic; space group no. 71, *Imma* = 14.42 (7) Å, *b* = 24.50 (4) Å, *c* = 11.72 (8) Å, *V* = 4140 Å³, *Z* = 2, *p*(calcd) = 1.455 g cm⁻³, crystal dimensions 0.05 × 0.07 × 0.32 mm; Mo Kα radiation, λ = 0.71073 Å; Enraf-Nonius SPD-CAD4 diffractometer; *R* = 0.0883, *R_w* = 0.0995 for 2312 observed reflections *F_o*² > *σ*²(*F_o*²). An empirical absorption correction was applied. All calculations were carried out on PDP 8A and 11/34 computers with the Enraf-Nonius CAD 4-SDP programs as described previously: Bohling, D. B.; Gill, T. P.; Mann, K. R. *Inorg. Chem.* **1981**, *20*, 194. The dimen ligands in this structure were disordered,⁵ in a manner similar to that previously found.^{5a}

(12) Positional parameters are available as Supplementary Material. The full details of this structure will be published elsewhere.

(13) A very weak, second end point corresponding to a $\text{Ag}^+:\text{Ir}_2^{2+}$ ratio of 2:1 is also apparent in the titration curve (Figure 2). The equilibrium constant for the formation of this species is small and was ignored in our data analysis.

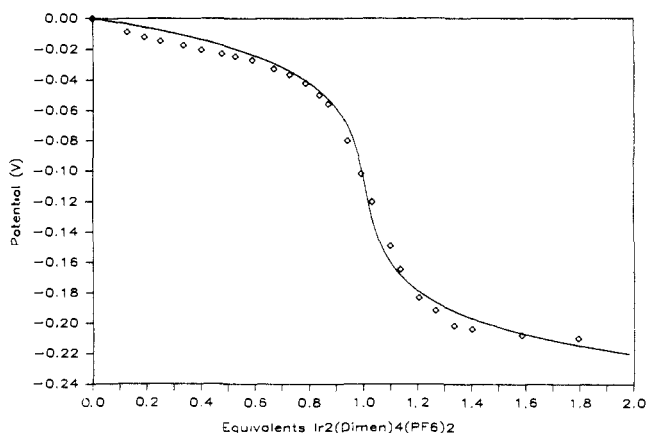


Figure 2. Potentiometric titration at 25 °C of a 3.67×10^{-4} M solution of AgPF_6 in DMSO with a 3.90×10^{-3} M solution of $\text{Ir}_2(\text{dimen})_4(\text{PF}_6)_2$. Ag wires were used as reference and indicator electrodes. An aliquot of the 3.67×10^{-4} M Ag^+ solution was used in the reference compartment. The curve is drawn for $K = 1.5 \times 10^8 \text{ M}^{-1}$ based on reaction 1.

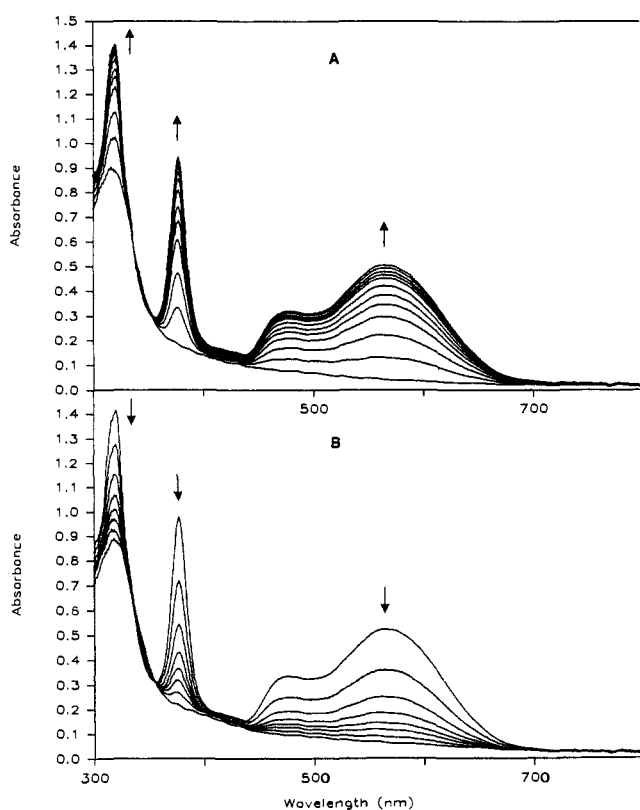
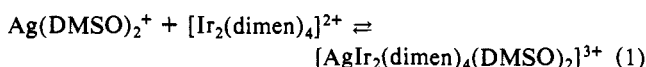


Figure 3. Arrows indicate the direction of absorbance changes. A. Photolysis (4 s between scans) with a 75 W Hg lamp of a CH_3CN solution of $[\text{AgIr}_2(\text{dimen})_4]^{3+}$ (1.3×10^{-4} M) and Ag^+ (1.0×10^{-4} M). B. Dark reaction (84 s between scans) of the solution produced in A after the photolysis is ceased.

a value for $\log K$ of 8.2. This corresponds to a free energy change of 4.8 Kcal/mol for the reaction



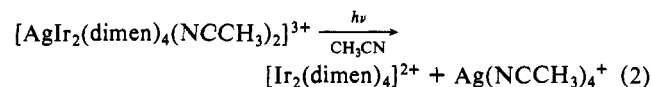
The magnitude of the encapsulation constant is similar to the binding of K^+ by 18-crown-6 ($\log K = 6.10$)¹⁴ and Cl^- by $\text{Ni}_2(\text{dimen})_4^{4+}$ ($\log K = 6.2$).^{5d} Comparisons with the Ni complex are particularly interesting because it has an encapsulated Lewis base (Cl^-) between two Lewis acids (Ni^{2+}), while the Ag^+ adduct

of $\text{Ir}_2(\text{dimen})_4^{2+}$ features the Lewis acid (Ag^+) between two Lewis bases (Ir^+). The substantial binding of the Ag^+ cation by two cationic Ir^+ centers illustrates the basicity and metal-metal bond-forming ability of the Ir^+ centers in $\text{Ir}_2(\text{dimen})_4^{2+}$.

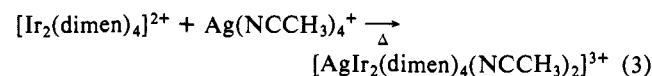
Perhaps the most interesting observations that we have made concerning the $[\text{AgIr}_2(\text{dimen})_4]^{3+}$ complex are long-lived emission¹⁵ from its fluid solutions and the rapid, reversible deencapsulation of the Ag^+ on exposure of $[\text{AgIr}_2(\text{dimen})_4]^{3+}$ to near UV light.

The emission spectrum of room temperature CH_2Cl_2 solutions of $[\text{AgIr}_2(\text{dimen})_4]^{3+}$ exhibits a bright orange emission¹⁶ centered at 640 nm. The emission maximum is considerably shifted from the position of the intense feature in absorption (390 nm), indicating that the emission is likely due to the corresponding spin forbidden process. This view is further substantiated by the long lifetime observed for the complex under these conditions. Measurement of the time dependence of the emission upon pulsed laser excitation of the complex gave clean exponential decays that were fit to the expression $I = I_0 \exp(-kt)$ with $k = 2.8 \times 10^5 \text{ s}^{-1}$ giving a lifetime of 3.6 μs . The lifetime observed for the ion in fluid solutions is long enough to allow bimolecular excited state processes. Further experiments to measure the temperature dependence of the emission lifetime and characterize the reactivity of the excited state are in progress.

Much weaker emission is observed for the $[\text{AgIr}_2(\text{dimen})_4]^{3+}$ ion in acetonitrile solutions. Under these conditions, continuous illumination (Figure 3A) causes the characteristic light yellow solution of $[\text{AgIr}_2(\text{dimen})_4(\text{NCCH}_3)_2]^{3+}$ to gradually darken to the purple color of the $[\text{Ir}_2(\text{dimen})_4]^{2+}$ parent complex.



This is a photochemical deencapsulation reaction that breaks both Ag^+-Ir^+ bonds to regenerate free Ag^+ . After illumination of the solution is discontinued, the purple color due to the parent $[\text{Ir}_2(\text{dimen})_4]^{2+}$ ion decreases, and the $[\text{AgIr}_2(\text{dimen})_4(\text{NCCH}_3)_2]^{3+}$ ion is regenerated (Figure 3B) in a slow thermal reaction.



This photochromic behavior can be repeated many times with the same solution and exhibits no apparent degradation. The photochemical deencapsulation reaction is remarkable in view of the large Ag^+ binding constant exhibited by the $[\text{AgIr}_2(\text{dimen})_4(\text{NCCH}_3)_2]^{3+}$ ion. An extensive study to determine the excited state binding constant of $[\text{Ir}_2(\text{dimen})_4]^{2+}$ for Ag^+ and the corresponding encapsulation/deencapsulation rates is in progress.

Acknowledgment. We thank Charles Daws for the lifetime measurements, Professors John Evans, Harold Swofford, Doyle Britton, and Harry Gray for several stimulating discussions, and Johnson-Matthew, Inc. for generous loans of rhodium and iridium trichloride.

Supplementary Material Available: Atomic coordinates for $[\text{AgIr}_2(\text{dimen})_4](\text{PF}_6)_3 \cdot 2\text{DMSO}$ and appendix (compound characterization) (5 pages). Ordering information is given on any current masthead page.

(15) Similar adducts that have the trimetallic $d^8-d^{10}-d^8$ electronic structure also show interesting luminescent characteristics: (a) Balch, A. L.; Nagle, J. K.; Olmstead, M. M.; Reedy, P. E., Jr. *J. Am. Chem. Soc.* **1987**, *109*, 4123. (b) Balch, A. L.; Nagel, J. K.; Oram, D. E.; Reedy, P. E. *J. Am. Chem. Soc.* **1988**, *110*, 454.

(16) $\text{Ir}_2(\text{dimen})_4^{2+}$ ion emits weakly in fluid solution but at considerably longer wavelengths ($\lambda_{\text{max}} = 710 \text{ nm}$). From the observed changes in emission and excitation spectra between $\text{Ir}_2(\text{dimen})_4^{2+}$ and $[\text{AgIr}_2(\text{dimen})_4]^{3+}$ we unambiguously concluded that both species emit in fluid solution. Qualitatively, $[\text{AgIr}_2(\text{dimen})_4]^{3+}$ is a stronger emitter than $\text{Ir}_2(\text{dimen})_4^{2+}$.

(14) Dietrich, B. *J. Chem. Ed.* **1985**, *62*, 954 and references therein.